

# Assessment of Microvascular Function Using Near-Infrared Spectroscopic 2D Imaging of Whole Hand Combined with Vascular Occlusion Test

Valentina Hartwig<sup>1</sup> · Martina Marinelli<sup>1</sup> · Fabrizio Rocco<sup>1</sup> · Antonio L'Abbate<sup>1,2</sup>

Received: 14 May 2015 / Accepted: 10 September 2015 / Published online: 30 January 2016  
© Taiwanese Society of Biomedical Engineering 2016

**Abstract** Near-infrared spectroscopy (NIRS) is an optical technique able to assess blood oxygen saturation (StO<sub>2</sub>) non-invasively. StO<sub>2</sub> of peripheral blood (blood contained in small vessels in strict contact with tissue cells) reflects the adequacy of blood flow and O<sub>2</sub> supply for tissue metabolism. Recent studies have tested the clinical utility of NIRS for studying peripheral microcirculation with the use of a NIRS probe, exploring a limited portion of hand skin (generally the thenar eminence), combined with vascular occlusion testing (VOT). In order to gain information from much larger tissue areas, the present study evaluates the possibility of using a NIRS two-dimensional (2D) camera for whole-hand imaging. Twelve healthy adults were tested. A NIRS camera was used to acquire the hemoglobin StO<sub>2</sub> 2D mapping of the whole-hand inner surface during VOT. Several parameters were calculated from the StO<sub>2</sub> trend obtained from the NIRS image set, using two exemplifying regions of interest on the thenar eminence and the middle finger.

**Keywords** Near-infrared spectroscopy (NIRS) · NIRS two-dimensional (2D) imaging · Skin microcirculation · Vascular occlusion test (VOT) · Microvascular diseases

## 1 Introduction

Adequacy of blood flow and thus of oxygen supply for tissue metabolic demand is fundamental for the viability and survival of an entire organism, single organ, or part of an organ. An imbalance between blood supply and oxygen need may result from systemic or regional diseases. Microcirculatory diseases may affect tissue oxygenation by functional and/or structural alterations of the small vessels (microvasculature) with very different distributions, variable diffusion, and progression in different patients and in different pathological conditions [1]. Microvessels distribute blood to all tissues, delivering oxygen and energetic substrates while removing products of catabolism. Vasomotricity (i.e., selective constriction or dilation) of different portions of the microvascular net, by complex local and/or systemic humoral and nervous control mechanisms, warrants the continuous fine matching between blood delivery and tissue metabolic demand. Alterations in the number and/or size of microvessels alter blood-tissue exchange, leading to temporary or permanent tissue damage. Functional microvascular alterations secondary to defects of vasomotricity are potentially reversible and sensitive to treatment, and generally precede structural alterations, which conversely lead to irreversible changes in vessel structure.

In the attempt to assess and identify microcirculatory alterations, several non-invasive techniques have been developed [1], including laser doppler flowmetry, which focuses on blood velocity across microvessels, echocolor-doppler, which can assess flow and morphology in medium-size digital arteries, plethysmography, which can assess total flow to the hand or single finger, and thermography, which is intended to provide indirect information on tissue perfusion and metabolism through

✉ Valentina Hartwig  
valeh@ifc.cnr.it

<sup>1</sup> National Research Council (CNR) Institute of Clinical Physiology, Via Moruzzi 1, 56124 Pisa, Italy

<sup>2</sup> Institute of Life Sciences, Scuola Superiore Sant'Anna, Piazza Martiri della Libertà 33, 56127 Pisa, Italy

measurement of local temperature. Finally, nail-fold capillaroscopy allows the accurate morphological analysis of nail-fold capillaries [1–3]. None of these tools, however, has been accepted as the gold standard method for the investigation of microcirculation and, at present, they are used in different ways depending on the specific clinical question.

The level of  $O_2$  saturation of hemoglobin ( $StO_2$ ) in the peripheral blood (i.e., blood contained in the small vessels (microcirculation) in strict contact with the tissue cells) reflects the tissue  $O_2$  content and in this sense its estimation can be very useful as a “sensor” of microcirculatory insufficiency, especially when normal  $O_2$  content can be assessed in the systemic arterial blood.

Recently, near-infrared spectroscopy (NIRS) has been proposed for the evaluation of tissue oxygenation and microcirculatory function. More specifically, NIRS has been used to evaluate the hand skin of healthy subjects [4–6] and for patients with peripheral vascular disease or sepsis [7–10].

NIRS utilizes near-infrared light to measure chromophores, including oxyhemoglobin ( $HbO_2$ ) and deoxyhemoglobin (Hb) [11]. The NIRS signal mainly derives from the blood hemoglobin contained in the small vessels embedded in the sampled tissue. By measuring changes in light absorption at different wavelengths, changes in tissue oxygenation can be measured in different physiological conditions. The relation between light absorption and concentration changes of chromophores is described by the modified Beer–Lambert law [12].

First described by Jobsis in 1977 [11], NIRS has been largely used for measuring changes in intravascular hemoglobin and intramuscular myoglobin for many applications [13–16]. First clinical applications of this technique principally focused on cerebral circulation [11, 17–19]. More recent studies have indicated the clinical relevance of NIRS measurement for superficial tissues. The NIRS technique has been used to quantify human skeletal muscle oxygen consumption [20, 21], blood flow [22, 23], and venous  $O_2$  saturation [24, 25]. Trends in human skeletal muscle deoxygenation have been studied during cuff ischemia and excessive exercise [26, 27]. Many studies have investigated peripheral vascular disease [28].

Generally, a NIRS probe that includes illumination and detection optical fibers is used. The probe uses reflectance mode to measure scattered light reflected at some distance from where the light was transmitted into the tissue. The probe is usually placed adhesively on the thenar eminence of the hand (i.e., thumb muscle) [29]. It has been demonstrated that adipose tissue thickness as well as the presence of edema can affect NIRS-derived measurements [20, 30].

The thenar eminence has thus been used in the majority of studies since it seems to be less influenced by edema with respect to other muscles and it less affected by adipose tissue differences between subjects [30]. Tissue oxygen saturation in the microvasculature of explored tissue is measured continuously and then the values are transferred to a computer and analyzed with dedicated software. In order to evaluate dynamic parameters in addition to resting  $StO_2$ , a vascular occlusion test (VOT) is performed. VOT involves inflating a pneumatic cuff around the upper arm in order to arrest blood circulation, keeping it inflated for a certain period, and then rapidly deflating it. During cuff inflation, the arterial and venous circulations are interrupted so that  $StO_2$  decreases, according to the consumption rate of the available  $O_2$  by the non-perfused tissue, until the circulation is restored after cuff deflation. The desaturation rate during ischemia (blood flow deprivation) and its reactive hyperemia (post-ischemia blood flow overshoot) represent tissue oxygen extraction and local small vessel dilation and recruitment, respectively [31]. The reoxygenation rate at reperfusion reflects the ability of the microcirculation to supply extra flow (reactive hyperemia), up to the restoration of the balance between blood inflow and tissue oxygen demand [8]. Based on their physiological meanings, all the above parameters derived from a sequence of  $StO_2$  images during VOT might be of diagnostic utility for patients affected by various vascular diseases [32, 33].

The aim of the present study was to test the feasibility of using NIRS two-dimensional (2D) whole-hand imaging combined with VOT to evaluate microcirculatory dysfunction, in the perspective of its potential use in a clinical setting. A NIRS camera (Kent Camera, Kent Imaging Inc., Calgary, Canada) was used to acquire the oxygen saturation 2D maps of the inner surface of the whole hand. As compared to existing techniques for the clinical investigation of microvascular diseases, NIRS whole-hand imaging has the significant advantage of allowing the study of large portions of skin tissue (dozen of square centimeters vs. a few square millimeters). This is particularly important, for example, in the case of collagen diseases, where microvascular alteration is, at least initially, limited to patchy and unpredictable areas of the microvascular network. An additional substantial advantage of NIRS is the nature of the biological variable measured (i.e., the hemoglobin  $O_2$  saturation of the portion of vascular blood pool that exchanges  $O_2$  with tissue). This parameter better reflects the metabolic state of the tissue, the most clinically relevant information, as compared to the other parameters such as blood flow, blood velocity, and capillary density provided by alternative techniques.

## 2 Materials and Methods

### 2.1 2D NIRS Imaging

This work used a NIRS camera (Kent Camera, Kent Imaging Inc.) to acquire the oxygen saturation 2D maps of whole-hand superficial tissues. This camera is a non-invasive tissue oxygenation measurement system that reports the value of StO<sub>2</sub> calculated starting from the HbO<sub>2</sub> and Hb levels in tissue. It is based on an array of 5-mm-diameter light-emitting diodes (LEDs) with four wavelengths (670, 730, 890, and 940 nm) and a charge-coupled device (CCD) sensor. The LEDs are distributed randomly within a rectangular area approximately 190 mm × 115 mm. Allowing for the central clear area of diameter approximately 35 mm at the CCD sensor location, the total area of the LED array is about 200 cm<sup>2</sup>. Individual LEDs are located on 7 mm centers in a hexagonal close-packed array. The total numbers of LEDs for wavelengths of 670, 735, 890, and 940 nm are 48, 30, 120, and 272, respectively. As stated by the manufacturer, the penetration depth of the NIR light is approximately 3 mm, so the camera permits the measurement of StO<sub>2</sub> in subcutaneous tissues [34]. The camera is mounted on a routable head (190 mm × 115 mm) at the extremity of an articulated arm. The camera can produce, in less than one second, the 2D color-coded image of tissue oxygenation of the scanned surface and reports multi-spectral tissue oxygenation measurements for selected tissue regions. Using a touch-screen, immediately after acquisition, the user may visualize the StO<sub>2</sub> value in any region of interest (ROI). The acquired images can be exported in DICOM standard format for further analysis. Each image has a resolution of 750 × 480 pixels.

### 2.2 Subjects

We enrolled twelve healthy volunteers (6 females, 6 males, 26 ± 3 years old, non-smokers) in this study. This study was done at the Institute of Clinical Physiology and was approved by our Institutional Review Board. Informed consent was obtained from all volunteers. A pre-participation questionnaire confirmed the absence of any known diseases. None of the volunteers were on vasoactive medication. The main characteristics of these volunteers are reported in Table 1 as the mean ± standard deviation (SD) (minimum–maximum). NIRS images were acquired on the non-dominant hand (i.e., left hand for all subjects). Subjects were requested to refrain from consuming caffeine-containing beverages for 12 h prior to the experiment. Before starting the test, the subjects rested in a comfortable position for at least 5 min, sitting with the forearm leaning on the table and the palm facing up. Room

**Table 1** Main characteristics of study subjects

Characteristic	Healthy volunteers (n = 12)
Age (years)	26 ± 3 (22–33)
Gender (male/female)	6/6
Height (m)	1.70 ± 0.10 (1.56–1.83)
Weight (kg)	65 ± 11 (49–79)
Body mass index (kg/m <sup>2</sup> )	22 ± 2 (20–26)
Systolic pressure (mmHg)	115 ± 15 (83–138)
Diastolic pressure (mmHg)	73 ± 10 (59–91)

temperature was carefully maintained during each experiment at 20 °C.

### 2.3 Experimental Protocol

NIRS oxygen saturation images of the non-dominant hand were acquired for all subjects during VOT. To this purpose, a pneumatic cuff was positioned around the upper arm and inflated with a sphygmomanometer to > 50 mmHg above the baseline systolic arterial pressure, measured at the beginning of the session. Testing consisted of 5 min of occlusion and 7 min of reperfusion. NIRS images were acquired at baseline, during 5 min of ischemia (blood flow cessation), and during 7 min of reperfusion. Four images were acquired at the baseline condition. During both ischemic and reperfusion phases, images were acquired every 10 s in the first minute and every 30 s thereafter. A total of 40 images were acquired for each subject. The total duration of each test (including preparation time) was about 30 min.

### 2.4 Image Post-processing

For further analysis of NIRS images, we developed a home-made tool using IDL (Version 8.0, Exelis Visual Information Solutions, Boulder, CO, USA). Using a graphical interface, the user was able to select any number and size of ROIs, calculate predefined parameters in each ROI, and save the results. Figure 1 shows two example ROIs selected in this study: ROI 1 on the thenar eminence and ROI 2 on the middle finger.

For each ROI, the mean StO<sub>2</sub> value (mean of pixels' values) was calculated at each time. Figure 2 shows a typical trend of StO<sub>2</sub> obtained during the experimental protocol. During the ischemic phase, the StO<sub>2</sub> level slowly decreased until its minimum value. Generally, after the cuff release, StO<sub>2</sub> rapidly increased and remained stable for a couple of seconds at the maximum value. Finally, it slowly returned to baseline values (Fig. 2). From the StO<sub>2</sub> curve, several parameters were calculated:

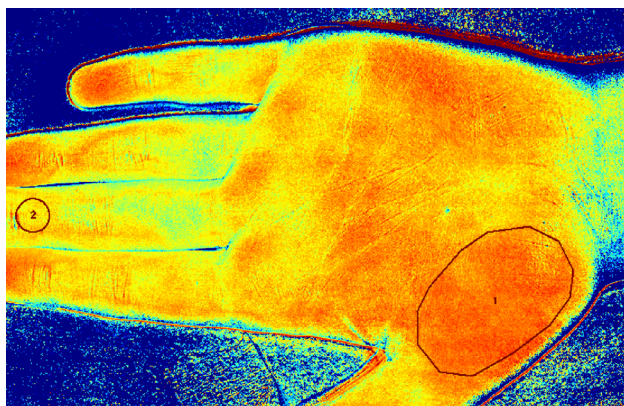


**Fig. 1** Selected ROIs for image processing

- (1) Baseline  $\text{StO}_2$  (%): averaged from the four pre-VOT values
- (2) Minimum  $\text{StO}_2$  (%): at the end of the ischemic phase
- (3) Descending rate (oxygen consumption rate) (%/min): an index of the tissue metabolism confronted with local  $\text{O}_2$  store [31]. It is defined by the regression line of the decrease in  $\text{StO}_2$  during the first minute after cuff inflation
- (4) Ascending rate (reperfusion rate) (%/s): it depends on the dilating response of microvasculature to ischemia and in particular reflects the integrity and functionality of the vascular endothelium [8]. It is defined by the regression line of the increase in  $\text{StO}_2$  after the cuff deflation
- (5) Hyperemic area (%\*min): the area under the curve above the baseline value, after the deflation of the pneumatic cuff. It reflects the hyperemic response, as confronted to  $\text{O}_2$  tissue re-payment, and can be used as an estimate of vascular dilation [5, 35]. It is calculated as the definite integral of the  $\text{StO}_2$  values

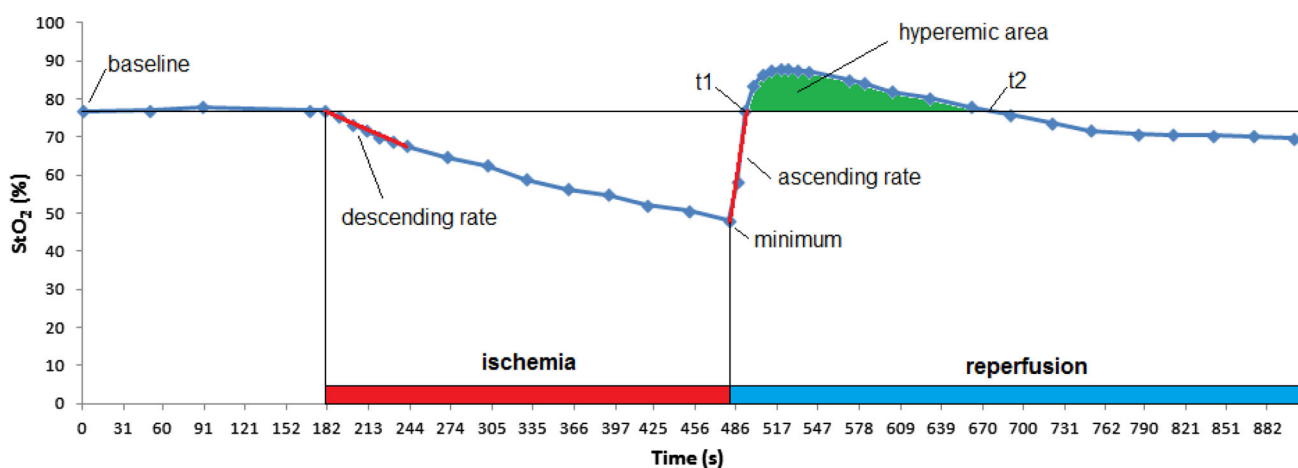
exceeding the baseline value during reperfusion (from  $t_1$  to  $t_2$  in Fig. 2) using a five-point Newton–Cotes integration formula. The time taken for oxygen saturation recovery after cuff deflation did not result superimposable for all subjects, being in some longer than the experimental session; in such instances, the hyperemic area was not calculated.

All variables are expressed as the mean  $\pm$  SD. Variables were tested for normality using the Lilliefors normality test. Afterward, all variables calculated respectively for thenar eminence and middle finger ROIs were compared using a  $t$  test for paired samples to assess statistical differences. Finally, a correlation analysis was performed between some variables on the thenar eminence ROI using Pearson's analysis. We considered  $p < 0.05$  to be significant.

### 3 Results and Discussion

Table 2 reports all the calculated variables from  $\text{StO}_2$  trends for the thenar eminence and the middle finger. Data are expressed as the mean  $\pm$  SD (minimum–maximum). The stars indicate variables that are significantly different between the thenar eminence ROI and the middle finger ROI (i.e.,  $p$  value  $< 0.05$ ). The area under the hyperemic curve was calculated for eight subjects only since four subjects did not reach the baseline value after 7 min of reperfusion.

Figure 3 shows five example NIRS images extracted from the 40-image series obtained for one healthy control. The color scale indicates the  $\text{StO}_2$  saturation in %. Figure 4 shows the  $\text{StO}_2$  (%) curves obtained during the experimental protocol in the two selected ROIs. Time 0 corresponds to cuff occlusion.

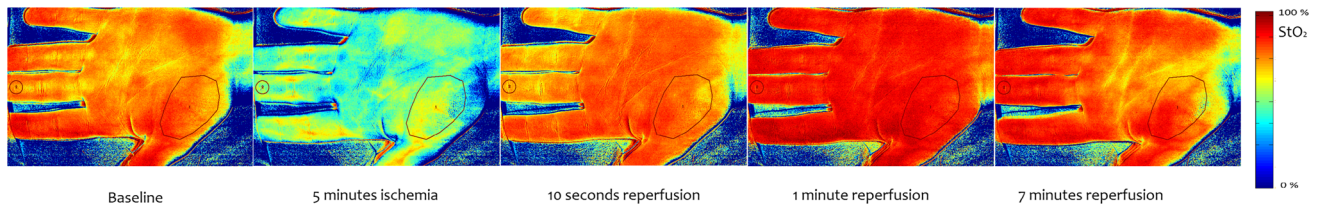
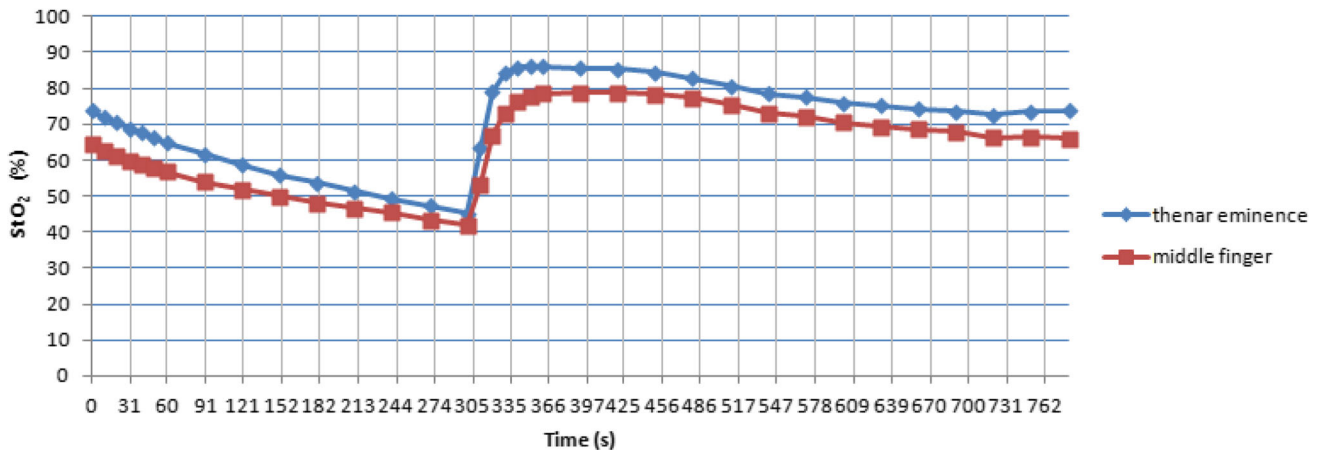


**Fig. 2** Trend of  $\text{StO}_2$  and calculated parameters



**Table 2** Tissue oxygen saturation curve variables in selected ROIs

Variables (n = 12)	Thenar eminence	Middle finger
Baseline StO <sub>2</sub> (%)	74.73 ± 6.55 (61.18–82.95)	65.34 ± 14.27 (25.81–79.59)*
Minimum StO <sub>2</sub> (%)	45.07 ± 10.98 (25.85–60.57)	41.8 ± 13.5 (5.66–55.18)
Descending rate (%/min)	−8.16 ± 1.80 (6.59–12.99)	−6.68 ± 1.62 (4.89–9.88)*
Ascending rate (%/s)	2.63 ± 0.55 (2.06–3.79)	1.98 ± 0.64 (0.98–2.74)*
Hyperemic area (% min) (n = 8)*	15.91 ± 6.79 (5.80–28.98)	32.98 ± 18.19 (16.98–59.69)*

\*  $p < 0.05$ **Fig. 3** Selected NIRS images of healthy subject. From left to right: baseline StO<sub>2</sub> image, end of ischemia, immediately after deflation of pneumatic cuff, 1 min after cuff deflation, and end of reperfusion phase**Fig. 4** StO<sub>2</sub> trend for each ROI: comparison between thenar eminence and middle finger

All the StO<sub>2</sub> variables had a normal distribution for both ROIs. The results of the *t*-test for paired samples, used to assess differences in variables between thenar eminence and middle finger ROIs, showed significant differences between baseline StO<sub>2</sub> ( $p = 0.0106$ ), descending rate ( $p = 0.0051$ ), ascending rate ( $p = 0.0079$ ), and hyperemic area ( $p = 0.0431$ ). The minimum StO<sub>2</sub> of the thenar ROI was not statistically different compared to that of the middle finger ROI. Figure 5 shows the individual values of the calculated parameters in thenar eminence and middle finger ROIs.

To investigate the relationship between the extent of ischemia and the StO<sub>2</sub> parameters of reperfusion and hyperemia, a correlation analysis (Pearson's analysis) was performed for minimum StO<sub>2</sub> versus the reperfusion parameter (i.e., StO<sub>2</sub> recovery slope) and hyperemic

parameter (i.e., hyperemic area). Moreover, the correlation between descending and ascending rates was determined in the thenar eminence ROI only.

StO<sub>2</sub> ascending rate was significantly correlated with the minimum StO<sub>2</sub> ( $n = 12$ ,  $r^2 = 0.4994$ ,  $p < 0.01$ ) while the area under the hyperemic curve was not ( $n = 8$ ,  $r^2 = 0.0653$ ,  $p > 0.05$ ). The descending rate was significantly correlated with the ascending rate ( $n = 12$ ,  $r^2 = 0.6869$ ,  $p < 0.001$ ).

Figure 6a shows the correlation curve between minimum tissue oxygen saturation and ascending rate (StO<sub>2</sub> recovery slope) in the thenar eminence ROI of healthy subjects. Figure 6b shows the correlation curve between the descending and ascending rates in the same ROI.

The aim of this study was to test in healthy volunteers the feasibility of using NIRS 2D whole-hand imaging

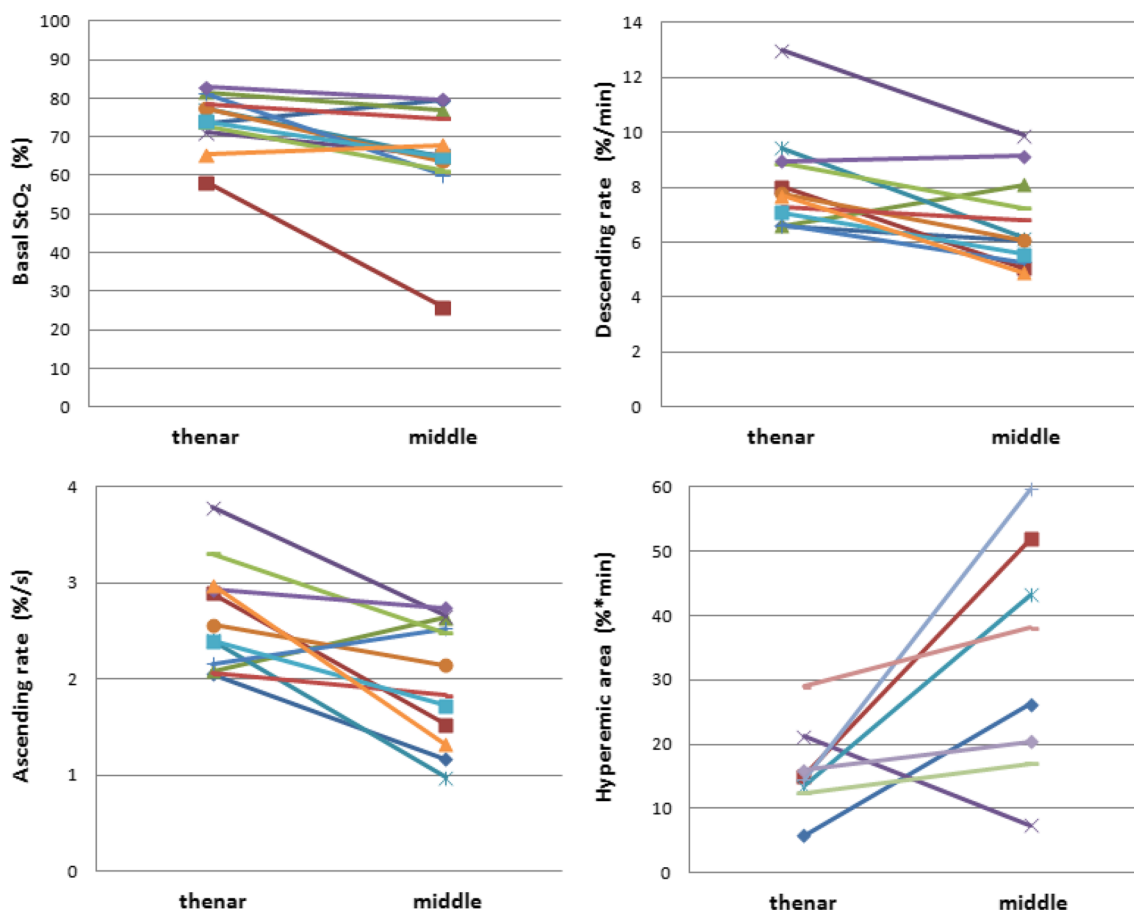


**Fig. 5** Individual values of calculated parameters in thenar eminence and middle finger ROIs

combined with VOT for the non-invasive assessment of microvascular function in a segment of the peripheral circulation (i.e., the hand) traditionally object of clinical interrogation in this respect. This was done in the perspective of a putative use of NIRS 2D in the workup of patients with overt or subclinical microvascular diseases.

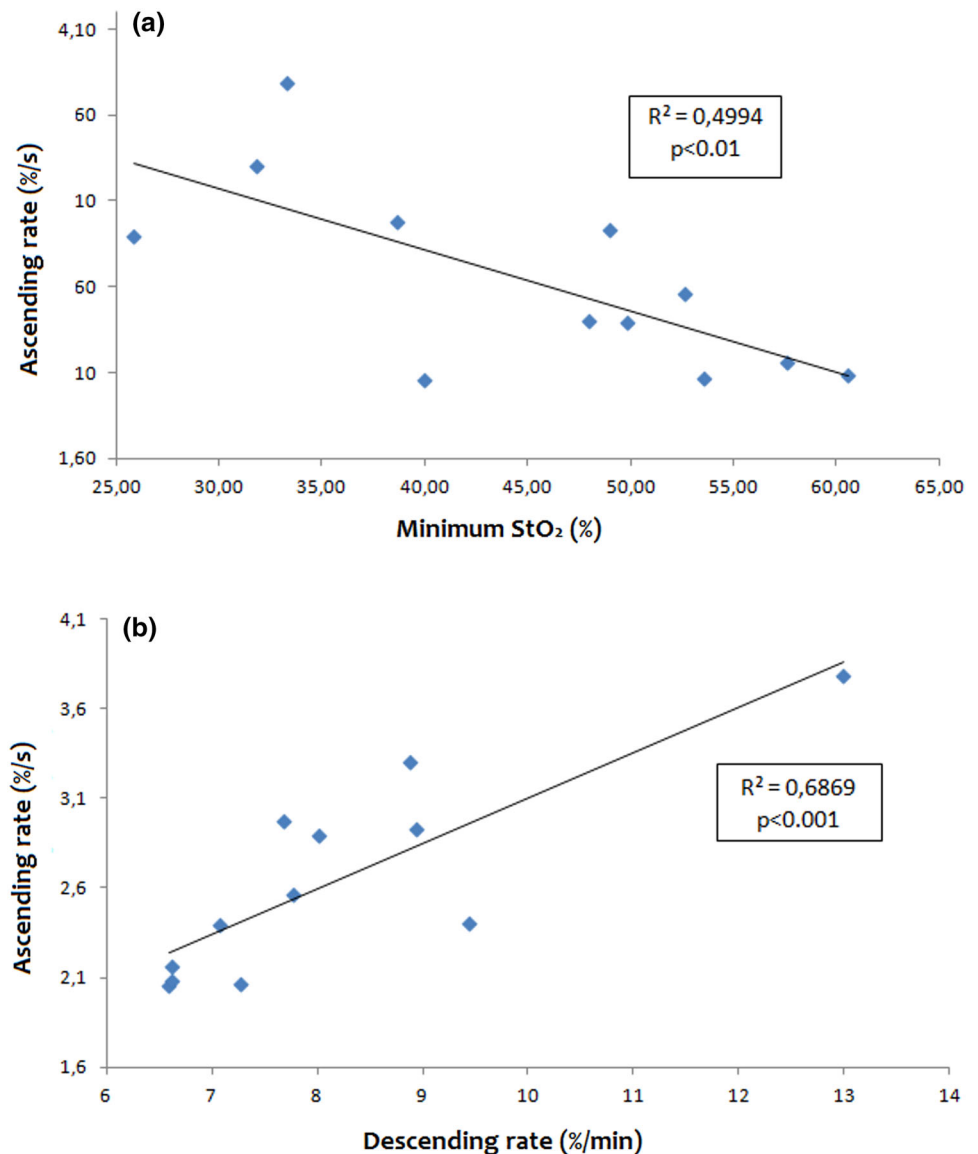
As microcirculatory alterations are frequently characterized by a very heterogeneous spatial distribution [1], it is easy to appreciate the potential of a diagnostic tool able to explore a large field of view with high spatial resolution. The utility of the NIRS approach for the assessment of hand skin microcirculation has been already demonstrated for patients with peripheral vascular disease [7] and sepsis [8–10]. However, to our knowledge, this is the first study on the use of NIRS 2D imaging in place of a topic spectrometer probe.

Studies in the literature conducted with various NIRS devices report very different results as NIRS measurements depend on the wavelength, number of wavelengths used, optode spacing, and algorithms used [36]. This absence of standardization limits comparisons of different trials. Moreover, various VOT protocols have been utilized, with

different duration of vascular occlusion and thus different severity of ischemic insult (3 or 5 min of occlusion or duration linked to a predefined minimum value of StO<sub>2</sub>, between 10 and 40 %). As StO<sub>2</sub> was not continuously measured in our study, the duration of ischemia was fixed rather than linked to a threshold StO<sub>2</sub> value. We chose a duration of 5 min, as all study participants were healthy and young. None of them reported discomfort during testing. For studies on patients affected by vascular diseases, a 3-min occlusion would likely be more appropriate in order to acquire all variables needed without inducing discomfort.

In our study, two ROIs were chosen in two different areas of the palm: the thenar eminence and the middle finger. The thenar eminence was chosen to compare our results with data in the literature and in particular to establish the feasibility of a dynamic test with an imaging device. Our results in the thenar ROI show lower values of StO<sub>2</sub> at rest as compared to the literature data for healthy subjects [5, 6, 10, 37]: this is probably related to the lower depth of light penetration of our system as compared to that of the spectrometer probe.

**Fig. 6** Correlation curves **a** minimum  $\text{StO}_2$  versus ascending rate in thenar eminence and **b** descending rate versus ascending rate in thenar eminence



Although in healthy subjects microcirculation heterogeneity is minimal [38], comparison of thenar eminence and middle finger ROIs showed statistically different values both at rest and during dynamic saturation changes. This finding underlines the importance of exploring a large portion of tissue, rather than tiny, generally single, samples [1].

#### 4 Conclusion

NIRS 2D imaging is a promising diagnostic tool, especially for patients with microvascular diseases typically characterized by heterogeneously distributed blood flow disorders, where some areas are deprived of oxygen while others are not [39]. In this regard, it is noteworthy that the number, size, and anatomical location of the ROIs chosen in the present study were by way of example but not limited

thereto. Any other number, size, and site of ROIs could have been selected from the same set of experimental data. Moreover, one should consider that preservation of pixel data allows unlimited re-analyses of the experimental data set, based on different anatomical criteria or comparison with novel acquisitions during the follow-up.

We found a negative correlation between minimum  $\text{StO}_2$  and  $\text{StO}_2$  ascending rate in the thenar eminence, demonstrating that the lower the oxygen saturation level is at the end of ischemia, the higher is the resaturation rate at reperfusion. Resaturation is the return of low values of  $\text{HbO}_2$  saturation toward normal (baseline) values; it indicates the restoration of normal  $\text{O}_2$  tension in the tissue. This result is in accordance with previous reports [6, 37, 40] and supports the view that the ascending rate (i.e., recovery slope) of  $\text{StO}_2$  following temporary blood cessation may well represent an index of microvascular function (i.e., the

physiological ability of the microvessels to dilate in response to metabolic challenges, to promptly restore tissue metabolic balance). Structural microvascular alterations as well as impairment of endothelial function can profoundly alter the vasodilation of microvessels.

The area under the hyperemic curve was not correlated with the minimum StO<sub>2</sub> value in our study. Only one study in the literature reported a significant correlation between these two variables [40]. With respect to this inconsistency, one should consider that the ‘recovery curve’ of StO<sub>2</sub> does not reproduce the hyperemic curve of blood flow, but is markedly dumped due to the fact that high saturation values (close to the upper limit of 100 %) do not reflect the actual increase in tissue perfusion, as is the case for values in the low range of the scale.

The descending rate of StO<sub>2</sub> had a strong positive correlation with the ascending rate of StO<sub>2</sub> in the thenar eminence. In the absence of flow, the descending rate of StO<sub>2</sub> reflects tissue consumption of available O<sub>2</sub>. The oxygen consumption rate has been used in the literature as an estimate of the basic metabolism of thenar muscle [4, 5]. The correlation we found for this variable with the ascending rate reasonably reflects the ability of microcirculation to dilate in response to ischemia, and could be used to document microvascular dysfunction.

The results of the present study allow us to state that the acquisition of whole-hand 2D map of hemoglobin oxygen saturation associated with the analysis of saturation changes in selected ROIs during VOT provides information on the functionality of the microvasculature and, importantly, on its spatial heterogeneity (information unavailable using existing clinical techniques). These findings, obtained for healthy volunteers, represent the basis for the clinical use of 2D NIRS in the workup of patients with suspected or overt microvascular disorders. It is important to stress that, different from existing techniques, the analysis of NIRS images can be applied at any time, without repeating the experiment, to different ROIs for differential diagnosis by region, or follow-up considerations on disease progression.

In conclusion, the results of this study support the use of NIRS hand imaging for the study of microcirculatory dysfunction. It is a non-invasive technique, easy to use, and reproducible, and might be a new tool for diagnosing microvascular dysfunction and evaluating its response to physical or therapeutic interventions.

## References

- De Backer, D., Ospina-Tascon, G., Sagado, D., Favory, R., Creteur, J., & Vincent, J. L. (2010). Monitoring the microcirculation in the critically ill patient: Current methods and future approaches. *Applied Physiology in Intensive Care Medicine*, 36, 1813–1825.
- Herrick, A. L., & Clark, S. (1998). Quantifying digital vascular disease in patients with primary Raynaud’s phenomenon and systemic sclerosis. *Annals of the Rheumatic Diseases*, 57, 70–78.
- Lima, A., & Bakker, J. (2012). Noninvasive monitoring of peripheral perfusion. In M. R. Pinsky, et al. (Eds.), *Applied physiology in intensive care medicine: Physiological reviews and editorials* (pp. 39–49). Berlin Heidelberg: Springer-Verlag.
- De Blasi, R. A., Cope, M., Elwell, C., Safoue, F., & Ferrari, M. (1993). Noninvasive measurement of human forearm oxygen consumption by near infrared spectroscopy. *European Journal of Applied Physiology*, 67, 20–25.
- Siafaka, A., Angelopoulos, E., Kritikos, K., Poriazzi, M., Basios, N., Gerovasili, V., et al. (2007). Acute effects of smoking on skeletal muscle microcirculation monitored by near-infrared spectroscopy. *Chest*, 131, 1479–1485.
- Lipsey, M., Eastwood, G. M., Woinarski, N. C. Z., Bellomo, R., & Care, C. (2012). Near-infrared spectroscopy of the thenar eminence: Comparison of dynamic testing protocols. *Critical Care and Resuscitation*, 14, 142–147.
- Ubbink, D. T., & Koopman, B. (2006). Near-infrared spectroscopy in the routine diagnostic work-up of patients with leg ischaemia. *European Journal of Vascular and Endovascular Surgery*, 31, 394–400.
- Creteur, J., Carollo, T., Soldati, G., Buchele, G., De Backer, D., & Vincent, J. L. (2007). The prognostic value of muscle StO<sub>2</sub> in septic patients. *Intensive Care Medicine*, 33, 1549–1556.
- Doerschug, K. C., Delsing, A. S., Schmidt, G. A., & Haynes, W. G. (2007). Impairments in microvascular reactivity are related to organ failure in human sepsis. *American Journal of Physiology Heart and Circulatory Physiology*, 293, H1065–H1071.
- Skarda, D. E., Mulier, K. E., Myers, D. E., Taylor, J. H., & Beilman, G. J. (2007). Dynamic near-infrared spectroscopy measurements in patients with severe sepsis. *Shock*, 27, 348–353.
- Jöbsis, F. F. (1977). Noninvasive, infrared monitoring of cerebral and myocardial oxygen sufficiency and circulatory parameters. *Science*, 198, 1264–1267.
- Kocsis, L., Herman, P., & Eke, A. (2006). The modified Beer-Lambert law revisited. *Physics in Medicine & Biology*, 51, 91–98.
- Jue, T., & Masuda, K. (2013). *Application of near infrared spectroscopy in biomedicine*. New York: Springer Science & Business Media.
- Lin, P., Lin, S., Penney, T., & Chen, J. (2009). Review: applications of near infrared spectroscopy and imaging for motor rehabilitation in stroke patients. *Journal of Medical and Biological Engineering*, 29, 210–221.
- Scott, J. P., & Hoffman, G. M. (2014). Near-infrared spectroscopy: Exposing the dark (venous) side of the circulation. *Paediatric Anaesthesia*, 24, 74–88.
- Ferrari, M., Muthalib, M., & Quaresima, V. (2011). The use of near-infrared spectroscopy in understanding skeletal muscle physiology: recent developments. *Philosophical Transactions of the Royal Society of London A: Mathematical, Physical and Engineering Sciences*, 369, 4577–4590.
- Wyatt, J. S., Cope, M., Delpy, D. T., Richardson, C. E., Edwards, A. D., Wray, S., & Reynolds, E. O. (1990). Quantitation of cerebral blood volume in human infants by near-infrared spectroscopy. *Journal of Applied Physiology*, 68, 1086–1091.
- Murkin, J. M., & Arango, M. (2009). Near-infrared spectroscopy as an index of brain and tissue oxygenation. *British Journal of Anaesthesia*, 103, 3–13.
- Ferrari, M., & Quaresima, V. (2012). A brief review on the history of human functional near-infrared spectroscopy (fNIRS) development and fields of application. *Neuroimage*, 63, 921–935.



20. Van Beekvelt, M. C., Colier, W. N., Wevers, R. A., & Van Engelen, B. G. (2001). Performance of near-infrared spectroscopy in measuring local O<sub>2</sub> consumption and blood flow in skeletal muscle. *Journal of Applied Physiology*, *90*, 511–519.
21. Binzoni, T., Cooper, C. E., Wittekind, A. L., Beneke, R., Elwell, C. E., Van De Ville, D., & Leung, T. S. (2010). A new method to measure local oxygen consumption in human skeletal muscle during dynamic exercise using near-infrared spectroscopy. *Physiological Measurement*, *31*, 1257–1269.
22. Edwards, A. D., Richardson, C., van der Zee, P., Elwell, C., Wyatt, J. S., Cope, M., et al. (1993). Measurement of hemoglobin flow and blood flow by near-infrared spectroscopy. *Journal of Applied Physiology*, *75*, 1884–1889.
23. Pichler, G., Urlesberger, B., Jirak, P., Zotter, H., Reiterer, E., Müller, W., & Borkenstein, M. (2004). Reduced forearm blood flow in children and adolescents with type 1 diabetes (measured by near-infrared spectroscopy). *Diabetes Care*, *27*, 1942–1946.
24. Yoxall, W., & Weindling, A. M. (1997). Measurement of venous oxyhaemoglobin saturation in the adult human forearm by near infrared spectroscopy with venous occlusion. *Medical & Biological Engineering & Computing*, *35*, 331–336.
25. Mozina, H., & Podbregar, M. (2010). Near-infrared spectroscopy during stagnant ischemia estimates central venous oxygen saturation and mixed venous oxygen saturation discrepancy in patients. *Critical Care*, *14*, R42.
26. Allart, E., Olivier, N., Hovart, H., Thevenon, A., & Tiffreau, V. (2012). Evaluation of muscle oxygenation by near-infrared spectroscopy in patients with Becker muscular dystrophy. *Neuromuscular Disorders*, *22*, 720–727.
27. Ambrozic, J., Lainscak, M., & Podbregar, M. (2013). Use of near infrared spectroscopy to assess remote ischemic preconditioning in skeletal muscle. *Physiology Journal*, *1–7*, 2013.
28. Vardi, M., & Nini, A. (2008). Near-infrared spectroscopy for evaluation of peripheral vascular disease. A systematic review of literature. *European Journal of Vascular and Endovascular Surgery*, *35*, 68–74.
29. Epstein, D., & Haghenbeck, K. T. (2014). Bedside assessment of tissue oxygen saturation monitoring in critically ill adults: An integrative review of the literature. *Critical Care Research and Practice*, *1–19*, 2014.
30. Poeze, M. (2006). Tissue-oxygenation assessment using near-infrared spectroscopy during severe sepsis: Confounding effects of tissue edema on StO<sub>2</sub> values. *Intensive Care Medicine*, *32*, 788–789.
31. Gómez, H., Torres, A., Polanco, P., Kim, H. K., Zenker, S., Puyana, J. C., & Pinsky, M. R. (2008). Use of non-invasive NIRS during a vascular occlusion test to assess dynamic tissue O<sub>2</sub> saturation response. *Intensive Care Medicine*, *34*, 1600–1607.
32. Parežnik, R., Knezevic, R., Voga, G., & Podbregar, M. (2006). Changes in muscle tissue oxygenation during stagnant ischemia in septic patients. *Intensive Care Medicine*, *32*, 87–92.
33. Payen, A., Luengo, C., Heyer, L., Resche-Rigon, M., Kerever, S., Damoiseil, C., & Losser, M. R. (2009). Is thenar tissue hemoglobin oxygen saturation in septic shock related to macrohemodynamic variables and outcome? *Critical Care*, *13*, S6.
34. Väiläso, P., Kaartinen, I., Tuchin, V., & Alander, J. (2011). New closed-form approximation for skin chromophore mapping. *Journal of Biomedical Optics*, *16*, 046012.
35. Gerovasili, V., Dimopoulos, S., Tzani, G., Anastasiou-Nana, M., & Nanas, S. (2010). Utilizing the vascular occlusion technique with NIRS technology. *International Journal of Industrial Ergonomics*, *40*, 218–222.
36. Boushel, R., & Piantadosi, C. A. (2000). Near-infrared spectroscopy for monitoring muscle oxygenation. *Acta Physiologica Scandinavica*, *168*, 615–622.
37. Mayeur, C., Campard, S., Richard, C., & Teboul, J. L. (2011). Comparison of four different vascular occlusion tests for assessing reactive hyperemia using near-infrared spectroscopy. *Critical Care Medicine*, *39*, 695–701.
38. Zuurbier, C. J., Van Iterson, M., & Ince, C. (1999). Functional heterogeneity of oxygen supply-consumption ratio in the heart. *Cardiovascular Research*, *44*, 488–497.
39. Goldman, A., Bateman, R. M., & Ellis, C. G. (2006). Effect of decreased O<sub>2</sub> supply on skeletal muscle oxygenation and O<sub>2</sub> consumption during sepsis: role of heterogeneous capillary spacing and blood flow. *American Journal of Physiology Heart and Circulatory Physiology*, *290*, H2277–H2285.
40. Bezemer, R., Lima, A., Myers, D., Klijn, E., Heger, M., Goedhart, P. T., et al. (2009). Assessment of tissue oxygen saturation during a vascular occlusion test using near-infrared spectroscopy: the role of probe spacing and measurement site studied in healthy volunteers. *Critical Care*, *13*, S4.